

Stationary population III accretion discs

Michael Mayer¹ and Wolfgang J. Duschl²

Institut für Theoretische Astrophysik, Tiergartenstr. 15, 69121 Heidelberg, Germany

¹ E-Mail: mm@ita.uni-heidelberg.de ² Email: wjd@ita.uni-heidelberg.de

14 December 2018

ABSTRACT

We present stationary models of protostellar population III (Pop III, for short) accretion discs, compare them to Pop I discs, and investigate the influence of the different chemical compositions on the occurrence of gravitational, thermal and thermal-viscous instabilities in the discs. In particular in the cooler regions, we find major differences between Pop III and Pop I discs, both in the structure and stability behaviour. This is mainly due to the absence of most molecules and dust in Pop III, which are very efficient absorbers in Pop I discs.

Key words: Accretion, accretion disks – hydrodynamics – Nuclear reactions, nucleosynthesis, abundances – Early Universe

1 INTRODUCTION

The important role of angular momentum during stellar and planetary formation is best evidenced by the remarkable co-planarity of the planetary orbits in our solar system. Observations of protostellar and protoplanetary accretion discs (Hartmann 1998) point towards this being generally the case. Even in the lack of direct evidence it is reasonable to assume that—as far as the role of angular momentum is concerned—the situation was not substantially different for the very first generation of stars, the population III (Pop III, for short).

While the general role of angular momentum may have been the same, and certainly will have led to the formation of population III accretion discs, the structure and the stability of these discs may have differed considerably from that of contemporary protostellar accretion discs. This difference in structure and evolution is not surprising given the difference in the chemical composition of accretion discs now (Pop I) and then (Pop III), in particular the lack of efficient cooling agents in the primordial matter discs.

Models of accretion in early universe so far assumed spherical accretion (Stahler et al. 1986). Only recently people started to work on accretion through a disc (Tan & McKee 2004, hereafter TM04). In particular, the importance of the opacity coefficient for the stability of accretion discs has been known for quite a while (e.g. Duschl 1993; Huré et al. 2001). In this contribution, we wish to investigate the structure and stability of population III accretion discs. For this purpose, we present stationary, vertically integrated, axially symmetric discs models.

In Sect. 2 we shall summarize the properties of the accretion disc model we used and present the set of equations solved. The subsequent Sect. 3 is dedicated to a short summary of the numerical method used to solve these set of equations. We then (Section 4) discuss the opacity coefficient for a Pop III chemical composition. Before we proceed to the presentation of the accretion disc models (Sect. 7), we shortly review criteria for thermal, thermal-viscous

and gravitational instabilities in Section 5 and give formulae for the timescales present in discs (Sect. 6) developing handy formulae for relevant limiting cases. We end in Sect. 8 with discussions of these results and put them into perspective.

2 THE ACCRETION DISC MODEL

We use a standard one zone accretion disc model (Pringle 1981) with slight but important modifications compared to the results of Mayer (2003): Our discs are allowed to be vertically self-gravitating and can become optically thin. Vertical self-gravity means that in a direction perpendicular to the rotational plane of the disc the gravitational acceleration is no longer restricted to be due to the projected contribution from the central object only, but now can also be due to the local mass distribution, or both at the same distance from the central object. The gravitational pull in radial direction is still only due to the central force as we exclude solutions where the disc mass becomes larger than the central mass, i.e. the rotational law is still Keplerian (KSG discs, Keplerian self-gravitating, see Duschl et al. 2000).

We have

- the continuity equation

$$\dot{M} = 2\pi r \Sigma u_r$$

- the angular momentum equation (ν viscosity; $f(r)$ accounts for the inner boundary condition, see eq. 7)

$$\nu \Sigma = \frac{\dot{M}}{3\pi} f(r) \quad (1)$$

- the energy equation

$$Q^+ = \frac{9}{8} \nu \Sigma \frac{GM}{r^3} = \frac{4\sigma}{3\tau_{\text{eff}}} T^4 = Q^- \quad (2)$$

It has been shown (TM04) that the ionisation energy may not be

2 Mayer & Duschl

neglected although the thermal energy is negligible. We do not account for this effect in our models (see discussion in Appendix D).

- hydrostatic equilibrium in vertical direction

$$\frac{1}{\rho} \frac{P}{H} = g_{c,H} + g_{KSG} = 2G \left(\frac{M}{4\rho r^3} + \pi \right) \Sigma \quad (3)$$

The pressure due to matter and radiation is sustained by the vertical component of the gravitational force $g_{c,H}$ of the central body and the vertical selfgravity of the disc ($g_{KSG} = 2\pi G\Sigma$, Paczynski (1978))

The optically thick \rightarrow optically thin transition is achieved by modifying the equation of state and the optical depth (Artemova et al. 1996)

$$P = P_g + P_r = \rho \frac{kT}{\mu m_p} + \frac{4\sigma}{3c\tau_{\text{eff}}} T^4 \left(\tau_R + \frac{4}{3} \right) \quad (4)$$

The effective optical depth is given by

$$\tau_{\text{eff}} = \tau_R + \frac{4}{3} + \frac{2}{3\tau_p} \quad (5)$$

where we define the Rosseland and Planck optical depth by

$$\tau_{R/P} = \frac{1}{2} \Sigma \kappa_{R/P}(\rho, T) \quad (6)$$

The radiation pressure reaches the black-body value $P = \frac{4\sigma}{3c} T^4$ for $\tau_{\text{eff}} = \tau_R \rightarrow \infty$ and is negligible in the optically thin regime ($\tau_R < 1$, $\tau_{\text{eff}} = \frac{2}{3\tau_p} \rightarrow \infty$, $\frac{\tau_R + \frac{4}{3}}{\tau_{\text{eff}}} \rightarrow 0$). In an optically thin medium photons are not able to contribute to the pressure in the gas as the mean-free path becomes long compared to the physical size of the medium they are passing through. The formal optical depth in eq. (5) which enters into the energy eq. (2) equals the usual diffusion approximation for $\tau_R \gg 1$ and moves into the optical thin regime for $\tau_R \ll 1$. In this respect we account for the transition from the optically thick diffusion approximation ($Q^- = \frac{4\sigma}{3\tau_R} T^4$) to the optically thin emission ($Q^- = 2\sigma T^4 \tau_p$).

The inner boundary condition ($\Sigma_{\text{in}} = 0$) can be expressed by

$$f(r) = 1 - \sqrt{\frac{r_*}{r}} \quad (7)$$

Once we are sufficiently away from r_* , $f(r) = 1$. For our models we set $f(r) = 1$. (see Sect. 7.1.1)

We furthermore define 2 parameters

$$\beta_p = \frac{P_g}{P_g + P_r} \quad \eta_{KSG} = \frac{g_{c,H}}{g_{c,H} + g_{KSG}} = \frac{M}{M + 4\pi\rho r^3}$$

β_p measures the contribution of the gas pressure to the total pressure ($\beta_p = 1$: pure gas pressure, $\beta_p = 0$: pure radiation pressure), and η_{KSG} the vertical selfgravity ($\eta_{KSG} = 1$: no vertical selfgravity, $\eta_{KSG} = 0$: fully vertically selfgravitating).

For the viscosity prescription we use α -viscosity (Shakura & Sunyaev 1973)

$$\nu = \alpha \frac{P}{\rho\Omega} \quad (8)$$

This corresponds to a stress tensor element $t_{r\phi} = -\alpha_p P$ with $\alpha_p = \frac{3}{2}\alpha$ which translates into the more commonly used $\nu = \alpha c_s H$ for the non-selfgravitating case. We use this more general viscosity prescription to avoid the difficulties of isothermality and rapidly increasing density in the vertically and fully selfgravitating parts of accretion discs when using $\nu = \alpha c_s H$ in all cases (Duschl et al. 2000)¹.

\dot{M}	accretion rate
Σ	Surface density $\Sigma = 2\rho H$
ρ	density
T	temperature
H	disc half thickness
ν	viscosity prescription
u_r	Radial drift velocity
Ω	Rotation frequency $\Omega_{\text{NSG/KSG}} = \sqrt{\frac{GM}{r^3}}$
P	pressure
c_s	sound speed
τ_{eff}	effective optical depth
M	central mass
r	radial distance
$\kappa_{R/P}$	Rosseland and Planck opacity
μ	mean molecular weight

Table 1. Nomenclature of the variables used. If not stated otherwise, the symbols refer to the disc's mid-plane

3 NUMERICAL TREATMENT

As we do not treat radial selfgravity and therefore have no implicit radial coupling, we are able to reduce the equations above into two equations depending only on density and temperature.

$$G \left(\frac{M}{4\rho r^3} + \pi \right) \left(\frac{\dot{M}}{3\pi\nu} \right)^2 = \rho \frac{kT}{\mu m_p} + \frac{4\sigma T^4}{3c\tau_{\text{eff}}} \left(\frac{\kappa_R \dot{M}}{6\pi\nu} + \frac{4}{3} \right) \quad (9)$$

$$\frac{3}{8\pi} \frac{GM\dot{M}}{r^3} = \frac{4\sigma}{3\tau_{\text{eff}}} T^4 \quad (10)$$

We solve these equations using a 2D nested intervals method for (ρ, T) in the range of $-16 < \log \rho < -2$ and $1.8 < \log T < 4.6$. We refine the initial rectangle 10 times so that we end up with an accuracy of $\Delta(\log \rho) \approx 0.02$ and $\Delta(\log T) \approx 0.003$.

In our system of equations we have left the effective optical depth τ_{eff} (given by eq. 5) and the viscosity ν . For the α -viscosity prescriptions it is impossible to explicitly calculate $\nu(\rho, T)$ as the radiation pressure depends on the surface density which itself depends on the viscosity. This implies a polynomial equation for ν of order 3. The details of this calculation are given in Appendix A. The optical depth still containing the surface density can be fully expressed in terms of density and temperature by using the angular momentum equation (1).

4 OPACITY

Primordial matter as an unprocessed relict from the big bang strongly differs from today's chemical composition as then the heavier elements which have to be produced first in stars were not present. Due to the lack of these metals, no dust could form. This lack of dust affects the opacities at low temperature, as dust is a very strong absorber.

In the absence of good absorbers unusual absorption effects become important: in the high-density and low-temperature regime collision-induced absorption (CIA) of H_2/H_2 , H_2/He , H_2/H and H/He -pairs dominates. In the low-temperature and low-density regime we have Rayleigh scattering in the Rosseland opacity while CIA continues to be the dominating effect in the Planck mean.

As there was no consistent and complete set of Pop III opacities available in the literature (except the ones of Lenzuni et al. from

¹ We note that in Duschl et al. (2000)'s notation the viscosity parametrization (8) corresponds to what they call the dissipation-limited case, i.e., where the turbulent velocity is limited by the sound velocity.

$P_g \gg P_r$	$\tau_R \gg 1$	$A_R - (1 + \eta_{KSG})B_R + 3(1 + \eta_{KSG}) < 0$
	$\tau_P \ll 1$	$-A_P + (1 + \eta_{KSG})B_P + 3(1 + \eta_{KSG}) < 0$
$P_r \gg P_g$	$\tau_R \gg 1$	$4A_R - \eta_{KSG}B_R - 4 < 0$
	$\tau_P \ll 1$	$-4A_P + \eta_{KSG}B_P - 4 < 0$

Table 2. Conditions for thermal instability

1000-7000 K and OPAL and OP ones above 10 000 K), we computed them on our own (Mayer, Diploma thesis; Mayer & Duschl, in prep.). The results are Rosseland and Planck mean opacities for $-16 < \log \rho < -2$ and $1.8 < \log T < 4.6$ assuming chemical equilibrium and only including continuum absorption (no lines). Our opacities match those of Lenzuni better than 10 % above 3000 K. Below 3000 K deviations are due to the implementation of CIA (e.g. Borysow et al. 1989)². The consistency with the OPAL and OP opacities is of the same level of accuracy, although we see larger differences in the high-density limit due to neglected pressure ionization.

During the last years it became widely accepted that it is sufficient to take hydrogen and helium species into account when dealing with Pop III matter. However there is a small number fraction of deuterium and lithium present, the latter of which must not be neglected.

Lithium belongs to the group of Alkali metals and can therefore easily be ionized. We included a simple deuterium and lithium chemistry. The deuterium chemistry does not affect the opacity at all, but the lithium changes the opacity up to two orders of magnitude due to its ability to provide free electrons at comparatively low temperatures. We do not include absorption effects of lithium and deuterium explicitly, lithium is only needed to alter the chemical equilibrium and therefore the absorption properties. The largest positive differences relative to the $Z = 0$ calculation occur at temperatures around a few 1000 K and at high and low densities while there is a negative difference at intermediate densities due to the destruction of H_3^+ .

Our opacity calculations show a difference between true Pop III and zero metallicity matter in this temperature range. Currently we only included continuum absorption of hydrogen and helium species with the exception of H_3^+ bound-bound transitions. Further details, a discussion of the opacity calculation and the inclusion of line absorption can be found in Mayer & Duschl (2004, in prep.). The models presented here were calculated with a Lithium fraction of $f_{Li} = 5 \cdot 10^{-10}$ and a Deuterium fraction of $f_D = 4 \cdot 10^{-5}$.

To compare with Pop I opacity we use the most recent compilation of low-temperature dust and gas opacities by Semenov et al. (2003).

5 STABILITY

5.1 Gravitational instability

The gravitational instability is usually characterized by the Toomre parameter (Toomre 1963):

$$Q = \frac{\Omega c_s}{\pi G \Sigma} \quad (11)$$

where we make use of $\kappa^2 = 4\Omega^2 + 2R\Omega \frac{d\Omega}{dR} = \Omega^2$ being the epicyclic frequency for Keplerian rotation. If $Q \ll 1$, then the disc might be

$P_g \gg P_r$	$\tau_R \gg 1$	$\frac{3A_R - (1 + \eta_{KSG})B_R + 5(1 + \eta_{KSG})}{A_R - (1 + \eta_{KSG})B_R + 3(1 + \eta_{KSG})} < 0$
	$\tau_P \ll 1$	$\frac{-3A_P + (1 + \eta_{KSG})B_P + 3(1 + \eta_{KSG})}{-A_P + (1 + \eta_{KSG})B_P + 3(1 + \eta_{KSG})} < 0$
$P_r \gg P_g$	$\tau_R \gg 1$	$\frac{12A_R + (2 - \eta_{KSG})B_R - 4(1 - 2\eta_{KSG})}{4A_R - \eta_{KSG}B_R - 4} < 0$
	$\tau_P \ll 1$	$\frac{-12A_P + (2\eta_{KSG} - 1)B_P - 4(2 - \eta_{KSG})}{-4A_P + \eta_{KSG}B_P - 4} < 0$

Table 3. Conditions for viscous instability

	$\left(\frac{\partial \log Q^+}{\partial \log T}\right) - \left(\frac{\partial \log Q^-}{\partial \log T}\right) =$	$\left(\frac{\partial \log \dot{M}}{\partial \log \Sigma}\right) =$
Ice grains	$(1 + \eta_{KSG})$	3
Evaporation of ice gr.	$10(1 + \eta_{KSG})$	$\frac{6}{5}$
Metal grains	$\frac{5}{2}(1 + \eta_{KSG})$	$\frac{9}{5}$
Evaporation of metal gr.	$1 + 27(1 + \eta_{KSG})$	$\frac{3 + 29(1 + \eta_{KSG})}{1 + 27(1 + \eta_{KSG})}$
Molecules	$\frac{2}{3}$	$6 + 3\eta_{KSG}$
H-scattering	$\frac{1}{3} - 7(1 + \eta_{KSG})$	$\frac{3 - 15(1 + \eta_{KSG})}{1 - 21(1 + \eta_{KSG})}$
Bound-free and free-free	$1 + \frac{1}{2}(1 + \eta_{KSG})$	$\frac{6 + 5(1 + \eta_{KSG})}{2 + (1 + \eta_{KSG})}$
Electron scattering ($\beta_P = 0$)	-4	$1 - 2\eta_{KSG}$

Table 4. Stability criteria (eqs. 12 and 13) evaluated for the fits to Pop I Rosseland mean opacities from (Bell & Lin 1994).

prone to axisymmetric instabilities leading to fragmentation. The true causes for low- Q discs are still under debate (e.g. see discussion in Goodman 2003).

5.2 Thermal instability

Suppose we got an equilibrium solution from eqns. 9 and 10. Then the disc is thermally unstable if an increase (decrease) of the heating rate is answered by a slower increase (decrease) of the cooling rate. In mathematical terms this criterion is given by

$$\left(\frac{\partial \log Q^+}{\partial \log T}\right)_P - \left(\frac{\partial \log Q^-}{\partial \log T}\right)_P > 0 \quad (12)$$

If we approximate the opacity by a power law depending on density and temperature $\kappa = C\rho^A T^B$, we can express the thermal instability condition (12) for limiting cases in terms of quantities depending on material functions only. We give the exact derivation in Appendix B. We summarize the most useful formulae in Table 2 (All cases for $\mu = \text{const}$).

5.3 Viscous instability

A disc is viscously unstable if an increase (decrease) of the local accretion rate is answered by a decrease (increase) of the surface density. Mathematically we can write this instability condition as

$$\left(\frac{\partial \log \dot{M}}{\partial \log \Sigma}\right)_P < 0 \quad (13)$$

We call a disc thermal-viscously unstable if it is thermally and viscously unstable.

For a power-law approximation of the opacity $\kappa_{R/P} = C_0 \rho^{A_{R/P}} T^{B_{R/P}}$ and $\mu = \text{const}$ we get the results shown in Table 3.

As an example we apply our instability criteria to the fits of Bell & Lin (1994) for Pop I chemical composition with $\tau_R \gg 1$,

² For an up-to-date reference of available CIA data see <http://www.astro.ku.dk/~aborysow/programs/>

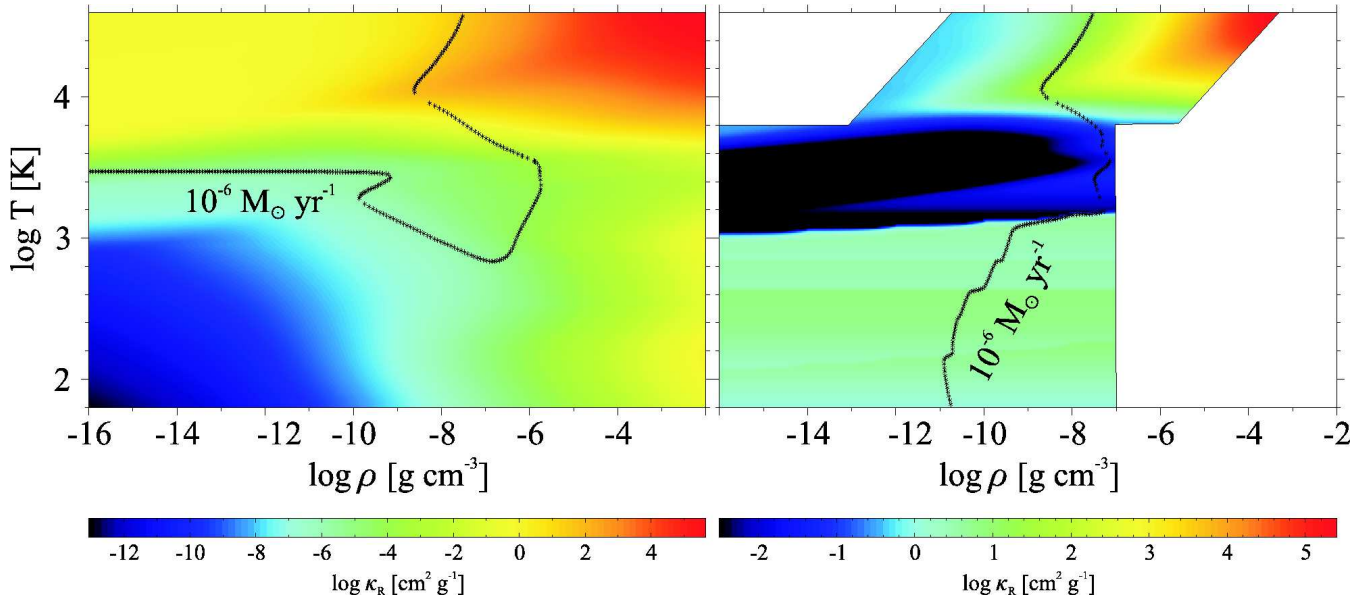


Figure 1. Sample accretion disc model for Pop III (left, Mayer & Duschl, 2004, in prep.) and today’s (right, Semenov et al. 2003) chemical composition for $\dot{M} = 10^{-6} M_{\odot} \text{yr}^{-1}$. Note the different colouring schemes mandated by the vastly different opacity range.

assuming gas pressure to be dominant ($\beta_p = 1$) except for Thomson scattering ($\beta_p = 0$), and show them in Table 4.

We see a thermal instability due to H-scattering and a thermal-viscous instability for electron scattering (for $\eta_{\text{KSG}} > 1/2$ only) This is the so called Lightman-Eardley instability (Lightman & Eardley 1974).

6 TIME SCALES

6.1 Viscous, thermal and hydrostatical equilibrium

The viscous, thermal and hydrostatic timescales are given by Pringle (1981).

$$\begin{aligned} \tau_{\text{visc}} &= \frac{r^2}{v} = \frac{r^2 \Omega}{\alpha c_s^2} \\ \tau_{\text{th}} &= \frac{\Sigma c_s^2}{Q^+} = \frac{\Sigma c_s^2}{\frac{9}{8} v \Sigma \Omega^2} = \frac{8}{9\alpha} \frac{1}{\Omega} \\ \tau_z &= \frac{H}{c_s} \end{aligned}$$

6.2 Chemical equilibrium

A cautionary remark when dealing with Pop III matter should be made regarding the chemical equilibrium. Due to the inefficient cooling compared to dust (The primary coolant being H_2), the only way to form H_2 in the low-density regime is via the H^- and H_2^+ channel (McDowell 1961; Peebles & Dicke 1968; Saslaw & Zipoy 1967). However in the high-density regime ($\rho > 10^{-16} \text{g cm}^{-3}$), three-body reactions rapidly convert neutral atomic into molecular hydrogen (Palla et al. 1983). A review describing chemical reactions in the early Universe can be found in Lepp et al. (2002). We calculated the H_2 formation timescale using the reaction rate k_4 of

Palla et al. (1983) (see Appendix C). We get in the disc geometry

$$\begin{aligned} \tau_{\text{H}_2} &= 0.51 \cdot \xi(M, \rho, r) \cdot \left(\frac{\alpha}{0.01}\right)^{-\frac{2}{3}} \left(\frac{\dot{M}}{10^{-4} M_{\odot} \text{yr}^{-1}}\right)^{\frac{2}{3}} \\ &\quad \cdot \left(\frac{M}{M_{\odot}}\right)^{\frac{1}{3}} \left(\frac{\rho}{10^{-8} \text{g cm}^{-3}}\right)^{-\frac{7}{3}} \left(\frac{r}{\text{AU}}\right)^{-1} \left(\frac{\mu}{1}\right)^2 \text{ s} \end{aligned}$$

$$\text{with } \xi(M, \rho, r) = 1 + 4.76 \left(\frac{M}{M_{\odot}}\right) \left(\frac{\rho}{10^{-8} \text{g cm}^{-3}}\right)^{-1} \left(\frac{r}{\text{AU}}\right)^{-3}$$

7 POPULATION III ACCRETION DISCS

7.1 Overall Properties

As we have seen in section 4, Pop III matter gives rise to unusual absorption mechanisms like CIA. Due to the lack of good absorbers it also cannot cool below a few 100 K (for an overview of the initial conditions used for collapse calculations see Ripamonti et al. 2002) with the only efficient coolant being mainly H_2 . This minimum temperature compared to the today’s value around 10 K implies larger Jeans masses (Clarke & Bromm 2003) and therefore larger accretion rates. Some authors conclude therefore that Pop III stars need to be more massive.

Fiducial values for primordial accretion discs are taken to be $\dot{M} = 10^{-4} M_{\odot} \text{yr}^{-1}$ compared to $\dot{M} = 10^{-6} M_{\odot} \text{yr}^{-1}$ for today’s accretion discs.

In our stationary accretion disc model the only parameters we can adjust are the central mass, the accretion rate, and the viscosity prescription. As standard value for α we use $\alpha = 10^{-2}$.

7.1.1 Self-similar solutions

For all models presented there is no specification of an inner boundary. In the scope of this paper, we want to keep the discussion as general as possible.

Equations (9) and (10) are two equations for the determinations of the density ρ and the temperature T at a given radial distance r , central mass M and accretion rate \dot{M} . However M and r are coupled in the sense that the equations yield the same result provided that $\Omega^2 = \frac{GM}{r^3}$, the rotation frequency is the same. Thus we present our disc models in terms of a generalised radial coordinate

$$\log q = \log\left(\frac{r}{1 \text{ AU}}\right) - \frac{1}{3} \log\left(\frac{M}{M_\odot}\right)$$

This approach only applies for NSG and KSG solutions. For the FSG(full-selfgravitating) case Ω also depends on the mass distribution of the disk itself.

For all models we choose a radial grid extending from $10^{-3} \dots 10^3 M_\odot^{-\frac{1}{3}}$ AU. At some accretion rates the inferred radius of the central star can be larger than our formal inner disc radius (e.g. see Fig.1 in Omukai & Palla 2001). The main scope of this paper is more on the global properties of Pop III accretion discs in comparison to Pop I discs. Therefore we do not specify any boundary conditions. This even makes the disk models applicable to primordial BH accretion.

Sample accretion disc models are shown in Fig. 1.

7.1.2 High-temperature limit

For high temperatures ($\log T \geq 3.8$) the models are nearly independent of metallicity, because at high temperatures the opacity is mainly dominated by hydrogen and helium species (up to an order of magnitude). And due to the $T^4/\tau_{\text{eff}} \propto \dot{M}\Omega^2$ proportionality a change in $\tau \propto \kappa_R$ by one order of magnitude changes the temperature only by a factor of 1.8 provided Σ remains constant.

7.1.3 Isothermal outer disc

One striking feature in the temperature $T(r)$ plot of Fig. 2 is the isothermal behaviour of the outer parts of Pop III discs. The temperature seems to be locked to approximately 3000 K. Inspecting the energy equation (2) and replacing τ_{eff} by $\frac{2}{3\tau_p}$ with $\tau_p = \frac{1}{2}\Sigma C_p \left(\frac{\rho}{\rho_0}\right)^{A_p} \left(\frac{T}{T_0}\right)^{B_p}$, we get:

$$T = T_0 \left(\frac{9\alpha k}{8\sigma T_0^3 C_p \mu m_p} \sqrt{\frac{GM}{r^3}} \left(\frac{\rho}{\rho_0}\right)^{-A_p} \right)^{\frac{1}{B_p+3}}$$

For all absorption effects the exponent A_p remains smaller than unity but the temperature dependence is far stronger. This is because at temperatures of a few 1000 K, H^- absorption is dominant. In the optical thin part (where Planck mean values apply) this absorption has a temperature dependence $B_p = \frac{\partial \log \kappa_p}{\partial \log T} \approx 20 \dots 30$. The high value of B_p ensures that then the exponent of the last equation is nearly zero and thus all radial dependencies vanish. The disc is isothermal in radial direction.

Such a temperature locking has also been shown for the spherical collapse calculations of Stahler et al. (1986) in the photosphere of the accretion shock of an evolving primordial star. Although the mechanism (H^- absorption) is the same, the isothermality for disk accretion is the property of the mid-plane temperature, while for spherical accretion this is evident in the photosphere of the evolving star.

Approximating the H^- opacity (neglecting density dependence, $A_p = 0$) we have

$$\kappa_{p,H^-} = C_p \left(\frac{T}{3000 \text{ K}}\right)^{B_p}$$

with $C_p = 10^{-8.4} \frac{\text{cm}^2}{\text{g}}$ and $B_p = 22$.

Following our argumentation above we get

$$T = 3440\text{K} \cdot \left[\left(\frac{\alpha}{0.01}\right) \left(\frac{M}{M_\odot}\right)^{\frac{1}{2}} \left(\frac{r}{\text{AU}}\right)^{-\frac{3}{2}} \right]^{\frac{1}{3+B_p}}$$

In today's accretion discs at 3000 K molecular opacities of H_2O and TiO soften the temperature dependence and therefore let the temperature decrease significantly. With decreasing temperature we get into the region of dust opacity which does not provide these steep temperature gradients.

7.1.4 Disc thickness

As one consequence of this radial isothermality in Pop III discs the relative disc thickness H/R increases as the disc is optically thin and $H/R = c_s/(\Omega r) (1 + \eta_{\text{KSG}}/(1 - \eta_{\text{KSG}}))^{\frac{1}{2}} \propto c_s/(\Omega r) \propto (Tr)^{\frac{1}{2}}$. For constant T we have $H/R \propto r^{\frac{1}{2}}$. This leads to the break-down of the thin-disc approximation as H/R reaches and exceeds unity. The other consequence is the radial decline of the surface density $\Sigma \propto r^{-\frac{3}{2}}$. We use the angular momentum equation (1) and get $c_s^2 \Sigma \propto \Omega \dot{M}$ and with isothermality $\Sigma \propto \Omega \propto r^{-\frac{3}{2}}$.

In the dust opacity disc models the temperature is not constant in the outer disc. Therefore H/R decreases with the onset of vertical selfgravity, as then $H/R \propto T/(\Sigma r) \approx T/r$.

7.1.5 Minimal temperature

Between the hot inner part and the isothermal outer part, stationary Pop III discs have an intermediate region, where the disc can cool below the 3000 K of the outer parts. This is mainly due to the onset of CIA absorption. But as the density decreases, CIA absorption gets less and less efficient (absorption coefficient proportional to the product of number densities of the contributing absorbers). At a certain point the absorption is so inefficient that the disc becomes optically thin and the absorption turns into optically thin emission. The temperature has to rise again until it reaches that of the temperature locked outer region. The minimal temperature decreases with increasing accretion rate as then more and more material is accreted. Therefore the densities get higher and so does absorption.

7.2 Instabilities

7.2.1 Gravitational instability

Figure 3 shows the Toomre parameter for Pop III and Pop I discs. While the Toomre parameter decreases monotonically for Pop I discs (as temperature does) there is a difference in the Pop III case. The temperature reaches a minimum value and so does the Toomre parameter.

With the analytical considerations of Sect. 7.1.4 we can write the Toomre parameter (11) for the optically thin isothermal outer region as

$$Q = 10.7 \left(\frac{\alpha}{0.01}\right) \left(\frac{\dot{M}}{10^{-4} M_\odot \text{yr}^{-1}}\right)^{-1} \left(\frac{T}{3440\text{K}}\right)^{\frac{3}{2}}$$

For accretion rates in excess of $1.07 \cdot 10^{-3} M_\odot \text{yr}^{-1}$ ($\alpha = 0.01$) the necessary condition for fragmentation is fulfilled in the Pop III case.

In isothermal regions the Toomre parameter depends only on radially constant quantities. The surface density Σ and the rotation

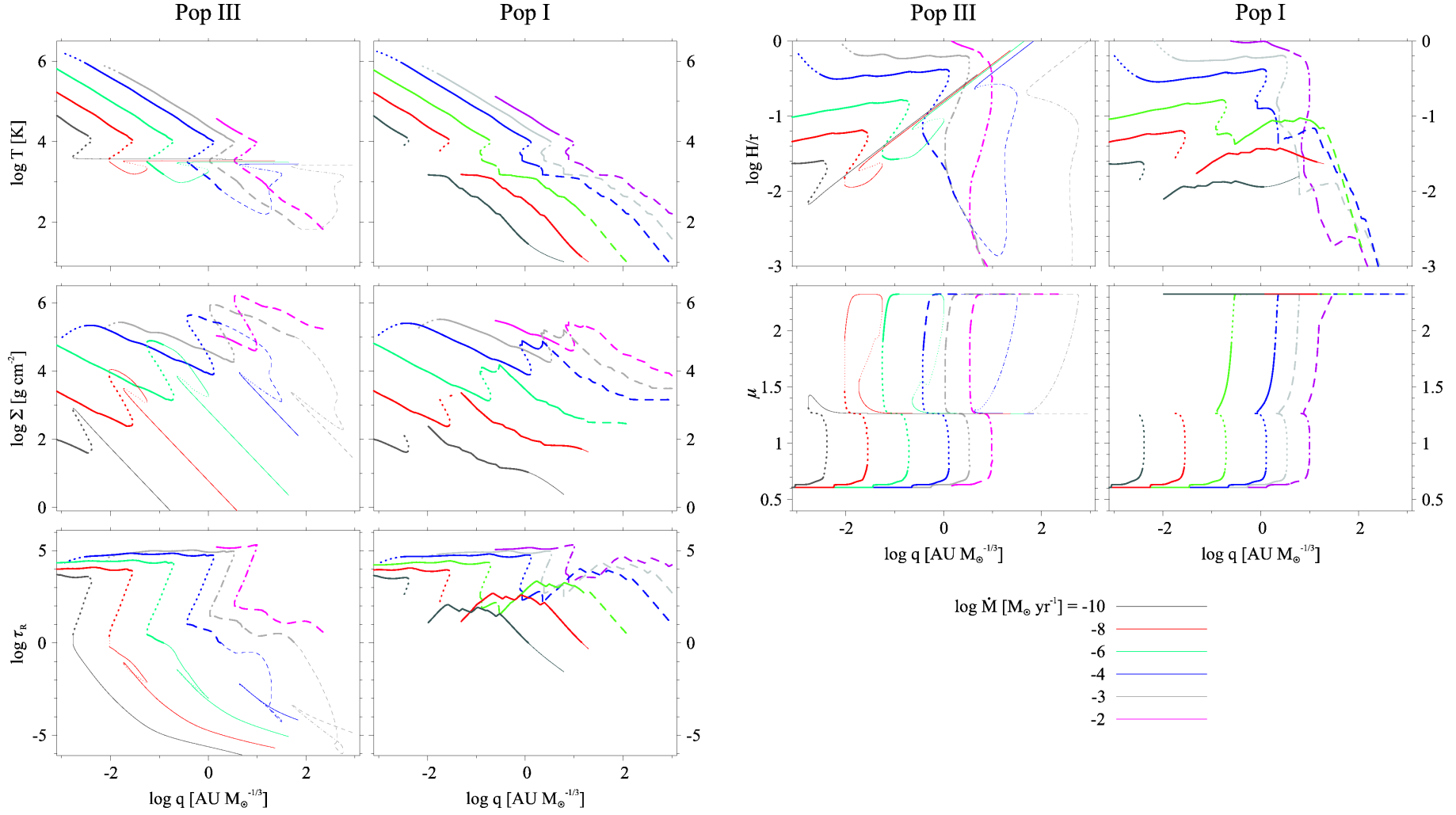


Figure 2. Comparison of the properties of discs with primordial and today's chemical composition: mid-plane temperature $T(r)$, surface density $\Sigma(r)$, Rosseland optical depth $\tau_R(r)$, relative thickness H/r , and mean molecular weight $\mu(r)$. Solid lines are stable solutions, dotted lines correspond to thermally unstable solutions and dashed lines are vertical selfgravitating solutions. Dash-dotted lines are vertical selfgravitating thermally unstable solutions.

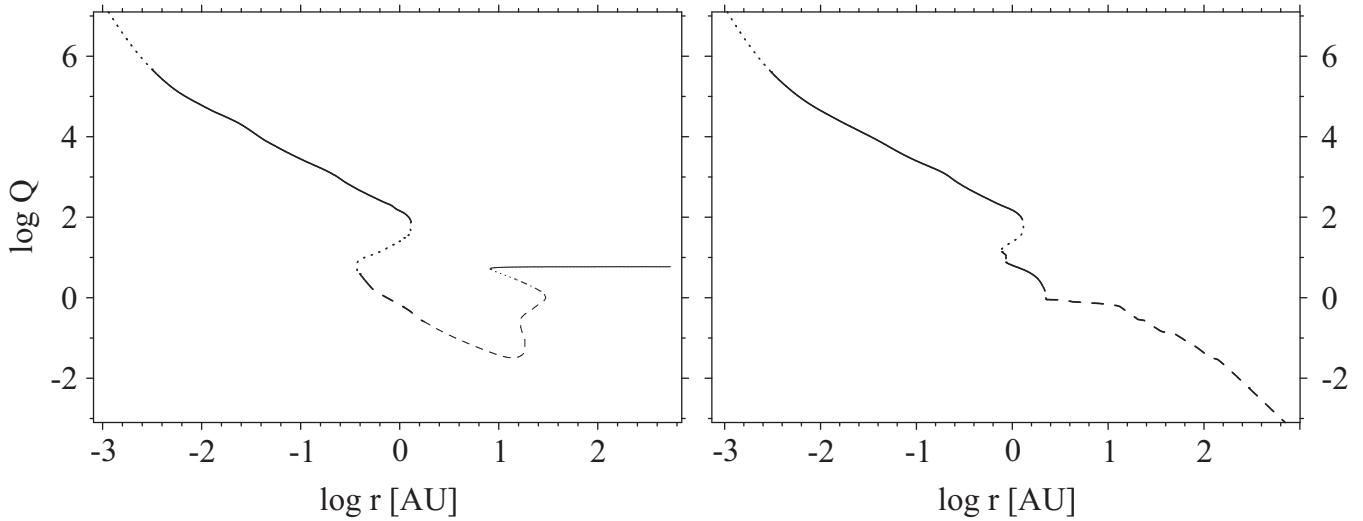


Figure 3. Toomre parameter Q for a accretion rate of $10^{-4}M_{\odot}\text{yr}^{-1}$ in disc models of Pop III (left) and Pop I (right) material. The disc is stable with respect to fragmentation for $\log Q > 0$.

frequency Ω both show the same radial dependence which cancels in eq. (11).

The maximum value of the viscosity parameter for marginally stable, selfgravitating discs is still a matter of debate: Tan & Blackman (2004) use $\alpha = 0.3$, following Goodman (2003), while Gammie (2001) finds analytically $\alpha \approx \frac{2}{90} \approx 0.022$ and numerically $\alpha \approx 0.0247$ (see his Sect. 4.1). By using $\alpha = 0.01$ we underestimate his critical accretion rate for fragmentation by a factor of order unity. Given the fact that the true critical Toomre parameter is still under debate (cf. Sect. 5.1), using $\alpha = 0.01$ seems to us to be adequate. Using $\alpha = 0.3$ for marginal selfgravity, as Tan & Blackman do, rises the critical accretion rate by a about one and a half orders of magnitude.

The role of selfgravity in Pop III is different compared to those found in Pop I. Usual low-temperature dust dominated Pop I discs become vertically selfgravitating (KSG) as the disc mass exceeds the fraction $\frac{h}{r}$ of the accreting mass and become fully selfgravitating (FSG) for disc masses larger than the accreting mass while remaining vertical selfgravitating (Duschl et al. 2000). However, in the Pop III case the outer parts can be FSG while not any more being KSG due to the local mass density.

This can be understood by examining the ratio

$$\frac{g_{\text{KSG}}}{g_{c,z}} = \frac{4\pi\rho r^3}{M}$$

For the Pop I case, due to cooling we have the decrease of the disc H/R ratio ($H/R \propto R^{-\xi}$, $\xi \approx 2$). With assuming the surface density $\Sigma \propto R^{-\zeta}$, $\zeta \approx 0$, the density is $\rho \propto \Sigma/H \propto R^{\xi-\zeta-1}$. The ratio $g_{\text{KSG}}/g_{c,z} \propto R^{\xi-\eta+2}$ increases with radius provided $\xi - \zeta > -2$ which is mostly satisfied in the Pop I case.

The scaling in Pop III is different. $H/R \propto R$ and $\Sigma \propto R^{-\frac{3}{2}}$ (see Sect. 7.1.4). Hence $\rho \propto \Sigma/H \propto R^{-\frac{7}{2}}$. Once the disc reaches the temperature-locked region (Sect. 7.1.3), $g_{\text{KSG}}/g_{c,H} \propto r^{-\frac{1}{2}}$. The vertical selfgravity is diminishing, while the disc mass in the isothermal part still increases. ($M_{\text{d, isothermal}} = \int 2\pi\Sigma r dr \propto r^{\frac{1}{2}}$).

Thus in the presence of Pop III matter one needs to distinguish between the local KSG-criterion ($g_{\text{KSG}}/g_{c,H} \geq 1$) and the global FSG-criterion $M_d \geq M$.

7.2.2 Thermal and viscous instabilities

In Fig. 2 we already indicate thermal instabilities. We now want to examine the effect of these instabilities by varying the accretion rate $\dot{M}(\Sigma)$ at given radial distance as shown in Fig. 4. According to eq. (13) the disc is viscously unstable for negative $\dot{M}-\Sigma$ slope. This is the case at very high accretion rates (Lightman-Eardley instability) in both chemical compositions and also at some kinks in the molecular opacities of Pop I material. In our Pop III disc models we do not find any viscous instabilities except at the turning points between the thermally stable and unstable solutions.

Fig. 4 shows that limit cycles are present. For both POP I and POP III matter the limit cycles are mainly due to H^- -absorption. The influence of molecular lines (TiO, CO, etc.), however, causes further kinks at lower accretion rates and prevents Pop I disks from undergoing large $\Delta\dot{M} - \Delta\Sigma$ outbursts. For POP III no such molecular lines are present at these temperatures (H_2 lines set in at lower temperatures). At the transition from the intermediate CIA cooled region of the disc to the isothermal outer disc there is an additional thermal instability present. This instability arises because at this temperatures H_2 dissociates while the contribution of atomic hydrogen to the opacity is not yet that large.

7.3 Timescales

For the assumptions in our disc model (hydrostatic, thermal and chemical equilibrium, 1+1D one-zone approximation) we need

$$\tau_{\text{visc}} \gg \tau_{\text{th}} \gg \tau_z \gg \tau_{\text{H}_2}$$

to be satisfied. We show the timescales for sample models in Fig. 5. The chemical equilibrium is implicitly assumed to be fulfilled everywhere except where we have a significant abundance of H_2 . In this domain we plot the H_2 formation timescale. Otherwise there are only ionic and/or ion-neutral chemical reactions which proceed on timescales much smaller than timescales present in the disc.

The assumption of chemical equilibrium is satisfied even in the Pop III case. The H_2 formation timescale is orders of magnitudes smaller than the vertical timescale except in the outer regions of the disc. As long as the density is high enough, the 3-body reactions rapidly convert atomic into molecular hydrogen. In the outer parts

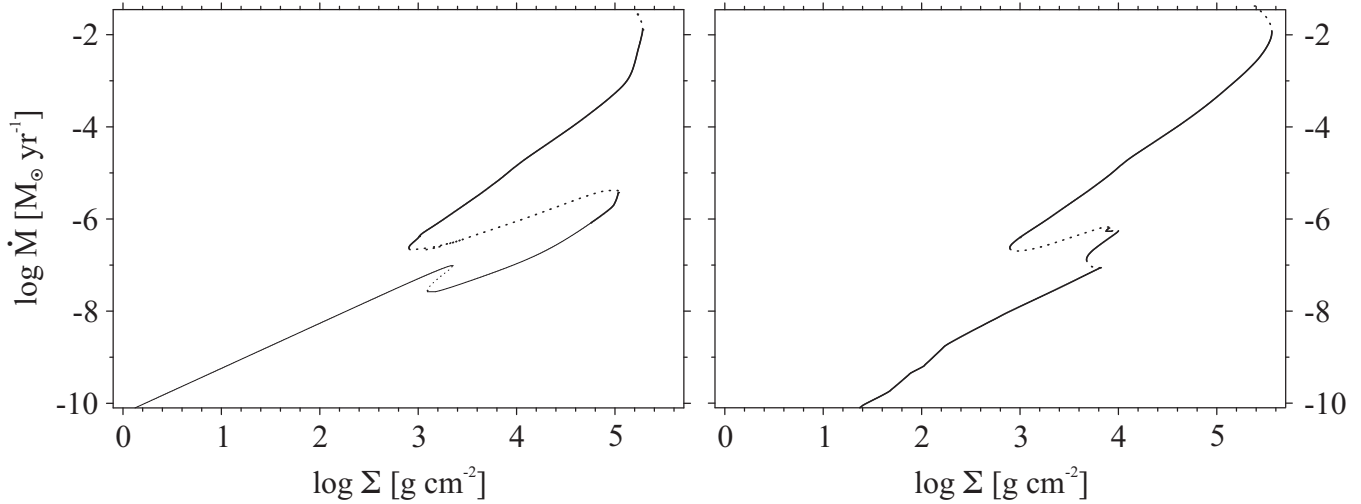


Figure 4. Accretion rate versus surface density at radial distance of $r = 0.1$ AU in disc models of Pop III (left) and Pop I (right) material with central mass of $1M_{\odot}$. The meaning of the lines, dots, etc. is the same as Fig. 2.

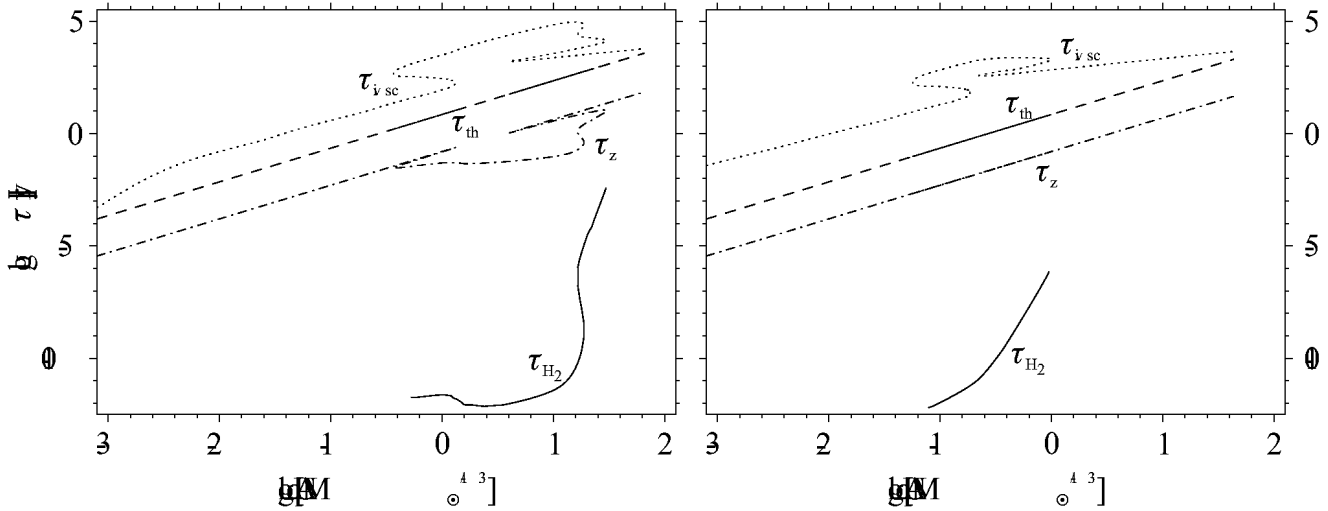


Figure 5. Timescales for Pop III disc models with accretion rates 10^{-4} (left) and 10^{-6} (right) $M_{\odot}\text{yr}^{-1}$.

of the disc, where τ_{H_2} increases, the strong density dependence of the 3-body reaction time scale can be seen.

However, our H_2 formation timescale should only be used with care. Our assumption is that this timescale equals the chemical reaction timescale. In general we only could assume that τ_{H_2} is a lower limit to the chemical reaction timescale as the consumed H still has to be depleted to reach chemical equilibrium.

As, however, τ_{H_2} is several orders of magnitude smaller than the hydrostatic timescale, atomic hydrogen has got time enough to be sufficiently depleted not influencing the opacity and therefore the disc structure. In the low-temperature region the only important absorption mechanism influencing the opacity is CIA.

The global maximum of the absorption coefficient normalized to standard number densities approximately coincide at the same level and the same frequency. Due to the quadratic dependence of the CIA on the density of the contributing species, once H_2 has been formed, CIA of H_2/H_2 pairs is the dominant absorption mechanism at high densities.

8 DISCUSSION

We have shown the impact of the different chemical composition on stationary accretion discs, comparing Pop III and Pop I material. This is mainly due to the lack of dust and heavier molecules (H_2O , TiO, etc.) absorption at low temperatures.

While the inner (hot) parts of Pop III discs do not largely differ from Pop I discs due to the dominant influence of hydrogen and helium species on the absorption, Pop III are optically thin and isothermal in their outer parts because of temperature locking due to H^- -absorption in the absence of dust. This leads to the breakdown of the thin-disc approximation as H/R increases proportional to $r^{\frac{1}{2}}$. Pop I discs do not have this locking mechanism. Therefore H/R decreases with the onset of the vertical selfgravity. This considerable flaring may lead to a disc structure modified by irradiation from the accreting star and the inner disc regions. Such effects, however, are beyond the scope of this paper.

The disk models considered in this paper do not take into account effects due to the inner or outer boundary condition. Thus for protostellar evolution the innermost solutions will be nonexis-

tent being part of the protostar, while the outer disk regions may be hidden in spherical accretion still ongoing (see TM04) .

At the very outermost parts of Pop III accretion discs the thermal timescale becomes larger than the viscous timescale as H/R reaches unity (see Fig. 5). However it remains to be shown whether the breakdown of the thin-disk approximation (Sect. 7.1.4) remains valid when taking into account irradiation.

The assumption of chemical equilibrium is well satisfied for all regions with reasonable disc solutions in contrast to primordial protostellar collapse models. Given the much smaller density, the H_2 formation timescale exceeds the dynamical time scale there.

Pop III discs have intermediate regions, where they are able to cool below the 3440 K of the outer temperature-locked zones, where CIA is the dominant absorption effect. The minimal temperature achievable decreases with increasing accretion rate. For accretion rates high enough these discs do have a vertically self-gravitating ring (see Fig. 2).

This self-gravitating ring may be subject to change after inclusion of line absorption in the opacity calculations. At low density and low temperature we expect primarily H_2 quadrupole line absorption which may prevent the disc from reaching the isothermal outer part. As the molecular lines are narrow and weak at low densities, the integrated absorption coefficient added to the continuum Planck opacities will become constant with decreasing density for given temperature ($\kappa_P(\rho, T) \propto T^A$), while it does not in the continuum case ($\kappa_P(\rho, T) \propto \rho T^B$). In this line absorption dominated regime, the Pop III opacities may exhibit the same behaviour as Pop I opacities do in their dust and ice dominated regime, although at much lower absolute values.

In this case, there may be at least two coexisting solutions: The isothermal part will remain (temperature is only fixed due to H^- absorption which will remain the dominant absorption in this temperature range) with the addition of a stable low-temperature solution branch.

As mentioned above, some authors conclude that Pop III stars must have been very massive. There have been many proposals of feedback phenomena which may halt the accretion (Omukai & Palla 2001, 2003). Our stability examinations show a direct limiting process. While with Pop I discs the accretion rate due to the thermal instability can be increased by 1.5 orders of magnitude in contrast to nearly 3 orders of magnitude for Pop III discs, Pop III discs are likely to exceed their Eddington Limit quite often and therefore produce massive outflows. However it remains to be shown in time-dependent simulations of Pop III discs how this instability acts.

The Toomre parameter of the isothermal outer region becomes lower than unity if the accretion rate exceeds $1.07 \cdot 10^{-3} M_\odot \text{yr}^{-1}$ (Sect. 7.2.1). While Tan & Blackman (2004) use $\alpha = 0.3$ (following Goodman (2003)) we use $\alpha = 0.01$ as the value for the viscosity parameter following Gammie (2001).

Discs well above this threshold accretion rate are certainly prone to fragmentation. Discs with lower rates can have Toomre parameter values $Q < 1$ in the intermediate regime but $Q > 1$ in the isothermal outer parts. This does not lead to fragmentation, as the viscous timescale in the outer parts of Pop III accretion disc decreases until the onset of the isothermal part. This means that the first stars can grow very large and that it is exceedingly hard to form Pop III planets.

ACKNOWLEDGEMENTS

The authors acknowledge support for this work from the *Deutsche Forschungsgemeinschaft, DFG* through grant *SFB 439 (A7)*. Part of this work was carried out while one of the authors (MM) stayed as an EARA Marie Curie Fellow at the Institute of Astronomy, University of Cambridge, UK. The hospitality of the IoA, and of Prof. J.E. Pringle in particular, is gratefully acknowledged. The authors thank Drs. Christian Straka and Franck Hersant for valuable discussions on the subject of this paper. Finally we thank the referee, Dr. Jonathan Tan for his comments on the manuscript, which helped to improve it.

REFERENCES

- Abel T., Bryan G. L., Norman M. L., 2002, *Science*, 295, 93
 Artemova I. V., Bisnovatyi-Kogan G. S., Bjoernsson G., Novikov I. D., 1996, *ApJ*, 456, 119
 Bell K. R., Lin D. N. C., 1994, *ApJ*, 427, 987
 Borysov A., Frommhold L., Moraldi M., 1989, *ApJ*, 336, 495
 Clarke C. J., Bromm V., 2003, *MNRAS*, 343, 1224
 Duschl W., 1993, in Greenberg J.M. Mendoza-Gómez C., Pirronello V., eds, *The Chemistry of the Life's Origin Vol. 55*, xyz. Kluwer, Dordrecht
 Duschl W. J., Strittmatter P. A., Biermann P. L., 2000, *A&A*, 357, 1123
 Gammie C. F., 2001, *ApJ*, 553, 174
 Goodman J., 2003, *MNRAS*, 339, 937
 Hartmann L., 1998, *Accretion Processes in Star Formation*. Cambridge University Press
 Huré J.-M., Richard D., Zahn J.-P., 2001, *A&A*, 367, 1087
 Lepp S. H., Stancil P. C., Dalgarno A., 2002, *Journal of Physics B Atomic Molecular Physics*, 35, 57
 Lightman A. P., Eardley D. M., 1974, *ApJ*, 187, L1+
 Mayer M., 2003, *Publications of the Yunnan Observatory*, 95, 151
 McDowell M. R., 1961, *Observatory*, 81, 240
 Omukai K., Palla F., 2001, *ApJ*, 561, L55
 Omukai K., Palla F., 2003, *ApJ*, 589, 677
 Paczynski B., 1978, *Acta Astronomica*, 28, 91
 Palla F., Salpeter E. E., Stahler S. W., 1983, *ApJ*, 271, 632
 Peebles P. J. E., Dicke R. H., 1968, *ApJ*, 154, 891
 Pringle J. E., 1981, *ARA&A*, 19, 137
 Ripamonti E., Haardt F., Ferrara A., Colpi M., 2002, *MNRAS*, 334, 401
 Saslaw W. C., Zipoy D., 1967, *Nature*, 216, 967
 Semenov D., Henning T., Helling C., Ilgner M., Sedlmayr E., 2003, *A&A*, 410, 611
 Shakura N. I., Sunyaev R. A., 1973, *A&A*, 24, 337
 Stahler S. W., Palla F., Salpeter E. E., 1986, *ApJ*, 302, 590
 Tan J. C., Blackman E. G., 2004, *ApJ*, 603, 401
 Tan J. C., McKee C. F., 2004, *ApJ*, 603, 383
 Toomre A., 1963, *ApJ*, 138, 385

APPENDIX A: THE IMPLICIT EQUATION FOR THE VISCOSITY

In the case of the α -viscosity the viscosity can be written as a function of density ρ and temperature T . We have

$$\begin{aligned} \nu &= \alpha \frac{P}{\Omega \rho} \\ &= \frac{\alpha}{\Omega} \left[\frac{kT}{\mu m_{\text{p}}} + \frac{4\sigma T^4}{3c\rho\tau_{\text{eff}}(\nu)} \left(\frac{\kappa_{\text{R}}\dot{M}}{6\pi\nu} + \frac{4}{3} \right) \right] \end{aligned}$$

making use of the angular momentum equation and

$$\begin{aligned} \tau_{\text{eff}} &= \frac{\kappa_{\text{R}}\dot{M}}{6\pi\nu} + \frac{4}{3} + \frac{4\pi\nu}{\kappa_{\text{p}}\dot{M}} \\ &= \frac{T_1 + T_2\nu + T_3\nu^2}{\nu} \end{aligned}$$

with

$$T_1 = \frac{\kappa_{\text{R}}\dot{M}}{6\pi} \quad T_2 = \frac{4}{3} \quad T_3 = \frac{4\pi}{\kappa_{\text{p}}\dot{M}}$$

and further setting

$$C_{\text{g}} = \frac{kT}{\mu m_{\text{p}}} \quad C_{\text{r}} = \frac{4\sigma T^4}{3c\rho} \quad C_0 = \frac{\alpha}{\Omega}$$

we get

$$\nu = C_0 \left[C_{\text{g}} + C_{\text{r}} \frac{T_1 + T_2\nu}{T_1 + T_2\nu + T_3\nu^2} \right]$$

$$\begin{aligned} T_3\nu^3 + (T_2 - C_0 C_{\text{g}} T_3)\nu^2 + (T_1 - C_0 T_2 (C_{\text{g}} + C_{\text{r}}))\nu \\ - C_0 T_1 (C_{\text{g}} + C_{\text{r}}) = 0 \end{aligned}$$

This equation has to be solved for given density and temperature.

APPENDIX B: THERMAL AND VISCOUS STABILITY OF RADIATIVELY SUPPORTED DISCS

In this section, variables like \bar{x} denote logarithmic variables.

We start with the equations for energy and hydrostatic equilibrium (see. eqns. 2 and 3)

$$\begin{aligned} \frac{9}{8}\nu\Sigma\Omega^2 &= \frac{4\sigma}{3c\tau_{\text{eff}}}T^4 \\ \rho \frac{kT}{\mu m_{\text{p}}} + \frac{4\sigma}{3c\tau_{\text{eff}}}T^4 \left(\tau_{\text{R}} + \frac{4}{3} \right) &= G \left(\pi + \frac{M}{4\rho r^3} \right) \Sigma^2 \end{aligned}$$

Using eqns. (4), (5) and (6) we can write ρ and T as a function of Σ . ν and τ_{eff} remain functions of ρ , T and Σ .

$$\rho(\Sigma) \quad T(\Sigma) \quad \tau_{\text{eff}}(\rho, T, \Sigma) \quad \nu(\rho, T, \Sigma) \quad (\text{B1})$$

B1 Viscous instability criterion

We are interested in the derivative

$$\left(\frac{\partial \dot{M}}{\partial \Sigma} \right)_{d\bar{Q}^+ = d\bar{Q}^-, d\bar{P} = 0} = \frac{\partial \dot{M}}{\partial \bar{\rho}} \frac{\partial \bar{\rho}}{\partial \Sigma} + \frac{\partial \dot{M}}{\partial \bar{T}} \frac{\partial \bar{T}}{\partial \Sigma} + \frac{\partial \dot{M}}{\partial \Sigma} \quad (\text{B2})$$

This derivative has to be calculated for equilibrium pressure and energy. Thus we have

$$\begin{aligned} d(\bar{Q}^+ - \bar{Q}^-) &= 0 \\ d(\bar{P}_{\text{g}} + \bar{P}_{\text{r}} - \bar{g}_{\text{c,H}}\Sigma + \bar{g}_{\text{KSG}}\Sigma) &= 0 \end{aligned}$$

which results in 2 linear equations for the unknown derivatives $\frac{\partial \bar{\rho}}{\partial \Sigma}$ and $\frac{\partial \bar{T}}{\partial \Sigma}$

$$\begin{aligned} A \frac{\partial \bar{\rho}}{\partial \Sigma} + B \frac{\partial \bar{T}}{\partial \Sigma} + C &= 0 \\ D \frac{\partial \bar{\rho}}{\partial \Sigma} + E \frac{\partial \bar{T}}{\partial \Sigma} + F &= 0 \end{aligned}$$

which can be calculated for $AE - BD \neq 0$ to

$$\frac{\partial \bar{\rho}}{\partial \Sigma} = \frac{BF - CE}{AE - BD} \quad \frac{\partial \bar{T}}{\partial \Sigma} = \frac{CD - AF}{AE - BD}$$

With a further examination of eq. (B2) we get

$$\begin{aligned} \left(\frac{\partial \dot{M}}{\partial \Sigma} \right)_{\text{p}} &= \frac{\partial \dot{M}}{\partial \bar{\rho}} \frac{\partial \bar{\rho}}{\partial \Sigma} + \frac{\partial \dot{M}}{\partial \bar{T}} \frac{\partial \bar{T}}{\partial \Sigma} + \frac{\partial \dot{M}}{\partial \Sigma} \\ &= \frac{\partial \bar{\nu}}{\partial \bar{\rho}} \frac{\partial \bar{\rho}}{\partial \Sigma} + \frac{\partial \bar{\nu}}{\partial \bar{T}} \frac{\partial \bar{T}}{\partial \Sigma} + \frac{\partial \bar{\nu}}{\partial \Sigma} + 1 \\ &= \frac{f(A, B, C, D, E, F, \frac{\partial \bar{\nu}}{\partial(\bar{\rho}, \bar{T}, \Sigma)})}{AE - BD} \\ \left(\frac{\partial \dot{M}}{\partial \Sigma} \right)_{\text{p}} &= \frac{f(A, B, C, D, E, F, \frac{\partial \bar{\nu}}{\partial(\bar{\rho}, \bar{T}, \Sigma)})}{AE - BD} < 0 \quad (\text{B3}) \end{aligned}$$

B2 Thermal instability criterion

Thermal instability requires

$$\left(\frac{\partial \bar{Q}^+}{\partial \bar{T}} \right)_{\text{p}} - \left(\frac{\partial \bar{Q}^-}{\partial \bar{T}} \right)_{\text{p}} > 0 \quad (\text{B4})$$

to be satisfied. We expand \bar{Q}^+ and \bar{Q}^- in terms of ρ and T

$$\begin{aligned} d(\bar{Q}^+ - \bar{Q}^-) &= \left(\frac{\partial \bar{Q}^+}{\partial \bar{\rho}} - \frac{\partial \bar{Q}^-}{\partial \bar{\rho}} \right) d\bar{\rho} + \left(\frac{\partial \bar{Q}^+}{\partial \bar{T}} - \frac{\partial \bar{Q}^-}{\partial \bar{T}} \right) d\bar{T} \\ &= A d\bar{\rho} + B d\bar{T} \end{aligned}$$

We further need to assure $d\bar{P}(\bar{\rho}, \bar{T}) = 0$

$$d(\bar{P}_{\text{c,H}} + \bar{P}_{\text{KSG}} - \bar{P}_{\text{g}} + \bar{P}_{\text{r}}) = D d\bar{\rho} + E d\bar{T} = 0$$

This is a condition which expresses $d\bar{\rho}$ in terms of $d\bar{T}$. We get our thermal instability condition according to eq. (B4) to

$$\left(\frac{\partial \bar{Q}^+}{\partial \bar{T}} \right)_{\text{p}} - \left(\frac{\partial \bar{Q}^-}{\partial \bar{T}} \right)_{\text{p}} = -\frac{AE}{D} + B > 0$$

As $D = \frac{\partial \bar{P}}{\partial \bar{\rho}} \geq 0$

$$AE - BD < 0 \quad (\text{B5})$$

The term $AE - BD$ is the same as in the denominator of the viscous instability criterion. Therefore it can be conjectured that if the disc is viscously unstable there also may be a thermal instability present. This leads to the expression of thermal-viscous instability. However this relation does not hold in a strict sense. There are at least formally possibilities having viscous instabilities without having thermal instabilities.

The conditions (B5) and (B3) can in principle be expressed now depending only on $A_{\text{R/P}}$, $B_{\text{R/P}}$, β_{p} and η_{KSG} with contributions of the μ -gradients in density and temperature. However we restrict

ourselves only to supply handy formulae for relevant limit cases. (See Section 5.2 and 5.3)

APPENDIX C: ESTIMATION OF THE H₂ FORMATION TIME SCALE

We calculate the disc properties analytically for a selfgravitating ring, assuming $\beta_p = 1$.

From the angular momentum equation (1) with the our viscosity prescription (8) we get

$$\dot{M} = 3\pi\alpha \frac{kT}{\mu m_p} \Sigma \sqrt{\frac{r^3}{GM}}.$$

This leads to

$$\Sigma(T) = \frac{\dot{M}\mu m_p}{3\pi\alpha kT} \sqrt{\frac{GM}{r^3}}.$$

Plugging this into the equation for the hydrostatic equilibrium leads to (3)

$$\rho \frac{kT}{\mu m_p} = G \left(\frac{M}{4\rho r^3} + \pi \right) \frac{\dot{M}^2 \mu^2 m_p^2}{9\pi^2 \alpha^2 k^2 T^2} \frac{GM}{r^3}.$$

This is an equation which can be solved for $T(\rho)$.

$$\begin{aligned} T^3 &= \left(\frac{M}{4\rho r^3} + \pi \right) \frac{\dot{M}^2 \mu^3 m_p^3}{9\pi^2 \alpha^2 k^3 \rho} \frac{G^2 M}{r^3} \\ T &= 2010 \text{ K} \cdot \xi(M, \rho, r) \cdot \left(\frac{\alpha}{0.01} \right)^{-\frac{2}{3}} \left(\frac{\dot{M}}{10^{-4} \text{ M}_\odot \text{ yr}^{-1}} \right)^{\frac{2}{3}} \\ &\quad \cdot \left(\frac{M}{\text{M}_\odot} \right)^{\frac{1}{3}} \left(\frac{\rho}{10^{-8} \text{ g cm}^{-3}} \right)^{-\frac{1}{3}} \left(\frac{r}{\text{AU}} \right)^{-1} \left(\frac{\mu}{1} \right)^1 \end{aligned}$$

with

$$\xi(M, \rho, r) = \left(1 + 4.76 \left(\frac{M}{\text{M}_\odot} \right) \left(\frac{\rho}{10^{-8} \text{ g cm}^{-3}} \right)^{-1} \left(\frac{r}{\text{AU}} \right)^{-3} \right)^{\frac{1}{3}}$$

With $k_4 = 1.83 \cdot 10^{-31} \left(\frac{T}{300\text{K}} \right)^{-1} \text{ cm}^6 \text{ s}^{-1}$ (Palla et al. 1983) and $\rho = \mu m_p n_{\text{H}}$ we get for the H₂ formation time scale:

$$\begin{aligned} \tau_{\text{H}_2} &= \frac{1}{2k_4 n_{\text{H}}^2} \\ &= 7.65 \cdot 10^{-2} \text{ s} \cdot \left(\frac{T}{300 \text{ K}} \right) \left(\frac{\rho}{10^{-8} \text{ g cm}^{-3}} \right)^{-2} \left(\frac{\mu}{1} \right) \\ &= 0.51 \text{ s} \cdot \xi(M, \rho, r) \cdot \left(\frac{\alpha}{0.01} \right)^{-\frac{2}{3}} \left(\frac{\dot{M}}{10^{-4} \text{ M}_\odot \text{ yr}^{-1}} \right)^{\frac{2}{3}} \\ &\quad \cdot \left(\frac{M}{\text{M}_\odot} \right)^{\frac{1}{3}} \left(\frac{\rho}{10^{-8} \text{ g cm}^{-3}} \right)^{-\frac{7}{3}} \left(\frac{r}{\text{AU}} \right)^{-1} \left(\frac{\mu}{1} \right)^2. \end{aligned}$$

Note : For $\xi = 1$ we are in the vertical selfgravitating domain, $\xi \geq 1$ elsewhere.

Alternatively we could have taken the reaction rate $k_{3b} = 1.3 \cdot 10^{-32} \left(\frac{T}{300 \text{ K}} \right)^{-1} \text{ cm}^6 \text{ s}^{-1}$ of Abel et al. (2002). Then the corresponding numerical factors would be 1.07 and 7.23. Using k_{3b} instead of k_4 leads to an order of magnitude higher value of τ_{H_2} .

However, with more and more H₂ being produced, another 3-body reaction (k_6 of Palla et al. 1983) will help in further reducing the formation time scale.

APPENDIX D: COMPARISON TO THE TAN & MCKEE (2004) DISC MODELS

TM04 present disc models for the inner regions of the accretion disc around a Pop III star. Their disc models span 1 decade in radial distance (with the exception of the 100 M_⊙ case), are strongly influenced by the inner boundary condition. In order to compare to our model, we subjected our discs to the same inner boundary. We present our results for two of their parameter sets in Fig. C1.

The results are very similar at the high-temperature region. However, the TM04 neglect the low-temperature region. Our models show that there are two stable solutions coexisting over large radial distances, connected through the thermally unstable part (cf. Fig. 2), giving rise to thermal instabilities.

TM04 further mention the importance of the ionisation term in the energy equation, while the thermal term is negligible. We do not account for this effect, as we want to keep the presentation as general as possible (see Sect. 7.1.1).

If there is any important term in the energy equation other than viscous dissipation and radiative losses, the discs are no longer geometrically thin disks. The hydrostatic equilibrium (3) reads

$$\frac{H^2}{r^2} = \frac{\Omega^2}{\Omega^2 + 4\pi G\rho} \cdot \gamma \cdot \frac{c_s^2}{u_\phi^2} = (1 - \eta_{\text{KSG}}) \cdot \gamma \cdot \frac{c_s^2}{u_\phi^2}$$

where $u_\phi = \Omega r$ is the azimuthal velocity, γ the adiabatic index, and $P = \gamma \rho c_s^2$ the speed of sound. Disks are thin ($H/R \ll 1$) as long as they are cool (thermal energy small compared to kinetic energy of the azimuthal flow). Disks become hotter to reach the same H/R ratio either for $\gamma < \frac{5}{3}$ (ionisation or dissociation present) or for $\eta_{\text{KSG}} > 0$ (see. $H/R(r)$ in Fig. 2 for the isothermal outer part of the $10^{-4} \text{ M}_\odot \text{ yr}^{-1}$ and $10^{-3} \text{ M}_\odot \text{ yr}^{-1}$). The first effect is present in the TM04 models whereas we set $\gamma = \text{const}$. However TM04 do not include vertical selfgravity which is the dominant vertical force at these high accretion rates.

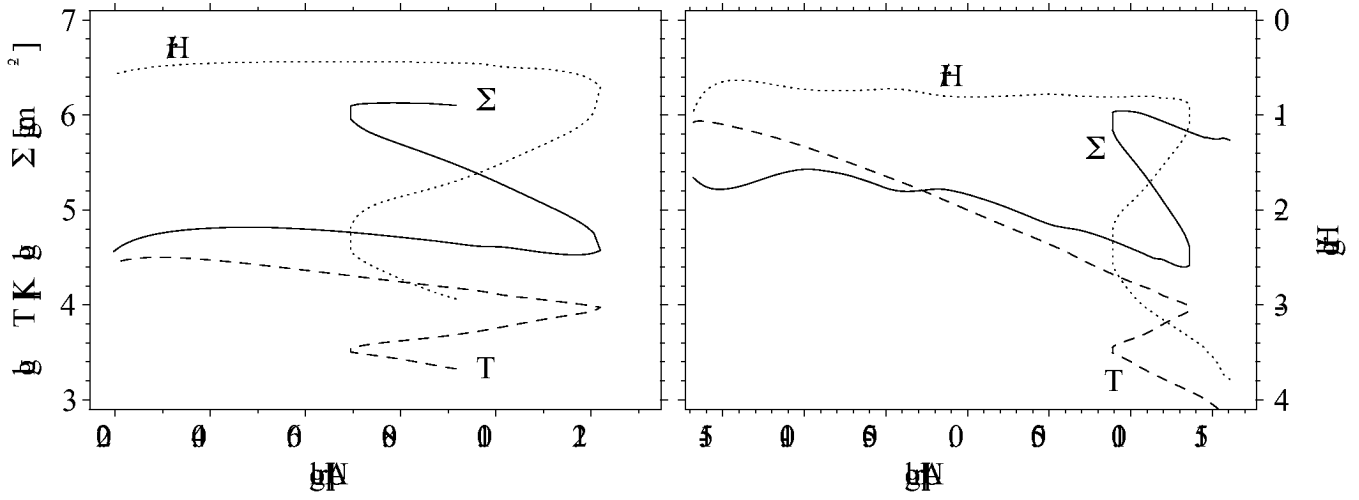


Figure C1. Accretion disc models for two cases of Tan & McKee (2004): $M = 10M_{\odot}$, $r_{*} = 300R_{\odot}$, $\dot{M} = 6.4 \cdot 10^{-3}M_{\odot}\text{yr}^{-1}$ (left), $M = 100M_{\odot}$, $r_{*} = 4R_{\odot}$, $\dot{M} = 2.4 \cdot 10^{-3}M_{\odot}\text{yr}^{-1}$ (right). α was chosen 0.01. We discard all solutions where Σs^2 , an approximation for the disc mass exceeds the central mass.